

## **Advanced Control of Ethylene to Butene-1 Dimerization Reactor**

**Emad Ali\* and Khalid Al-humaizi**

**Chemical Engineering Department, King Saud University**

**P.O.Box 800, Riyadh 11421, Saudi Arabia**

**Fax no.: ++(9661) 467-8770**

**Phone no.: ++(9661) 467-6871**

**Email address: amkamal@ksu.edu.sa**

### **Abstract**

Butene-1 is produced from ethylene by dimerization reaction in a CSTR. Due to the exothermic reaction, serious temperature runaway occurs in the reactor. Therefore, it is important to stabilize the reaction temperature in order to maintain good quality product and safe operation. Temperature stabilization is also essential for maintaining optimal operation of high ethylene conversion and desired butene-1 yield in the face of plant upsets. The objective of this paper is, thus, to study the simulated implementation of nonlinear control algorithms such as Fuzzy Logic Control (FLC), Globally Linearizing Control (GLC) and Nonlinear Model Predictive Control (NLMPC) algorithms for temperature stabilization of such a reactor to maintain favorable ethylene conversion and butene-1 yield conditions. The simulation results revealed the capability of all the proposed control algorithms to stabilize such a reactor with some differences in their performance. In addition, the performance of the nonlinear controllers outperforms that of the standard PI algorithm in terms of providing higher yield and shorter settling time during disturbances. However, careful tuning of the parameters of these controllers is necessary without which very aggressive or even unstable closed-loop performance will be obtained.

**Keywords:** Ethylene dimerization, Temperature stabilization, Fuzzy logic control, Globally linearizing control, Model predictive control

## **Introduction**

One of the most economic methods for producing butene-1 is the catalytic dimerization of ethylene. The reaction usually takes place at moderate pressure (20-30 psia) and temperature (50-60 °C). The catalyst used in the reaction is a homogeneous titanium-based catalyst, which leads to a high dimerization activity and excellent selectivity to butene-1. The industrial ethylene dimerization reactor operates in a liquid phase at bubble point conditions. Fresh ethylene and homogenous catalyst are fed continuously to the reactor where the exothermic reaction is removed by means of an external cooler. The cooler is installed on the recycle pipelines. The recycle returns portion of the product back to the reactor.

The ethylene dimerization process is strongly nonlinear and very sensitive to external disturbances. Thermal runaway risks are very common because the main reaction is highly exothermic and its rate increases rapidly with temperature. The side reactions produce heavier oligomers such as hexene and octene that might cause continuous fouling of the overall system of the reactor, recycle loop and heat exchangers. According to industrial practice, extreme regular monitoring of the process variables is necessary. Trabzoni (1998) has developed a mathematical model for this unit to study the static and dynamic behavior of such a reactor. The steady state analysis of the model shows that the system can exhibit a unique steady state and a multiplicity in the form of S shape (hysteresis). Generally, exothermic polymerization reactions with recycle are well known for reactor temperature instability (Dadebo, *et. al.*, 1997; Luyben, 1998). In fact, phases of variation such as persistent oscillation and/or runaway of the dimerization reactor temperature are reported (Braunschweig *et. al.*, 1990; Trabzoni, 1998). In fact, our previous work (Ali and Alhumaizi, 2000; and Alhumaizi, 2000) confirmed that the desired operating condition of maximum butene-1 yield occurs at an open-loop periodically unstable point. For this reason, control of the reactor temperature is essential for stable operations. In addition, good temperature control is important to maintain the process around the optimum conditions of maximum yield and to minimize large duration of off-specs products. The main objective of this paper is, thus, to design and test a good temperature controller.

Because the process is highly unstable, achieving a good control performance or even stable feedback response is a challenging task. Careful control design and tuning are essential

in this case to attain such control objectives. In fact, our earlier work (Ali and Alhumaizi, 2000) showed that implementation of a standard proportional-integral (PI) control algorithm and similarly a linear model predictive control algorithm can provide excellent control performance only at small magnitude for the disturbance. At large values for the disturbance, a multi-input multi-output (MIMO) control scheme, specifically 2x2 control loops, was found necessary to stabilize the reactor. However, the control performance was very sluggish. In addition, tuning of the MIMO scheme turned to be a difficult task. For these reasons non-linear control algorithms will be applied to control the reactor. Specifically, Fuzzy Logic Control (Lee, 1990a, 1990b), Globally Linearizing Controller (Kravaris et. al., 1989) and Nonlinear Model Predictive Controller (Ali and Zafiriou, 1993) will be used in this paper.

Fuzzy logic control is based on the original work of Zadeh (1965) on fuzzy set theory. Its first implementation to control physical processes was proposed by Mamdani (1974, 1977). Since then several other applications were reported (Bernard, 1988; Kishimoto et. al., 1989; Parekh et. al., 1994; Rhinehart et. al., 1996; Inmdar and Chiu, 1997; and Garrido et. al., 1997). Recently, FLC received more interest due to its successful application to important industrial systems (Rao, et. al., 1999). Since FLC is a nonlinear controller and can adapt itself to changing situations, it can outperform conventional PI controllers for unstable dynamics and nonlinear systems. In contrast to model-based controllers, FLC is known as a knowledge-based controller that does not require a mathematical model of the process at any stage of the controller design and implementation. In many cases, the phenomenological model of the control process may not exist or may be too expensive in terms of computer processing power and memory, and a system based on rules of human knowledge may be more effective. In this case, FLC is a simple alternative to model-based advanced controllers.

Globally linearizing controller is introduced first by Kravaris and Chung (1987) and belongs to a family of nonlinear control algorithms that uses the nonlinear model directly in the synthesis of the control law. It is also known as nonlinear internal model control (Kulkarni et. al., 1991; Patwardhan and Madhavan, 1998; Kendi and Doyle, 1998; Economu and Morari, 1986; Henson and Seborg, 1991; and Hu and Rangaiah, 1999), sometimes as output feedback control (Ramirez, 1999; Kumar and Daoutidis, 1995; and Alvarez, 1996) or input/output linearizing control (Alvarez et. al., 1994; Soroush and Kravaris, 1992). Most of these algorithms are based on the differential geometry technique and require analytical expression for the process model usually in the form of state space. Several simulated

implementation on nonlinear unstable models revealed the success of such a controller, which makes it suitable for our specific case. However, unlike other model-based controllers, GLC law formulation depends on the explicit analytical expression of the process model. This situation presents a barrier, which hindered the GLC implementation to real industrial control problems.

The nonlinear model predictive control belongs to the family of model predictive controllers (MPC). The MPC algorithms differ from the other advanced controllers in that a dynamic optimization problem is solved on-line each control execution. The original MPC uses a linear model in the form of step response and is known as dynamic matrix control (Cutler and Ramaker, 1979). Other generations of MPC were developed such as generalized predictive control (Clarke et. al., 1987) and quadratic dynamic matrix control (Garcia and Morshedi, 1986). Due to the MPC appealing features such as constraints handling and superiority for processes with large number of manipulated and controlled variables, it became the most widely used control system in the chemical industries (Qin and Badgwell, 1996; Morari and Lee, 1999). This success has led to the extension of MPC to consider nonlinear models for the online prediction (Ali and Zafiriou, 1993; Biegler and Rawlings, 1991). Review of the nonlinear MPC theory and its industrial applications has been reported (Henson, 1998; Qin and Badgwell, 2000).

Therefore, the specific objective of this paper is to investigate the simulated implementation of FLC, GLC and NLMPC to stabilize the dimerization reactor. The paper is organized as follows. The following section presents the mathematical model for the dimerization reactor and its cooling system followed by a section devoted for the open-loop analysis of the model. The fourth section discusses the control objectives of the dimerization reactor. The following three sections are devoted for the development of the proposed nonlinear controllers. The eighth section is devoted for illustrative closed-loop simulations. The last section offers the final conclusions.

## **Reactor Model**

The dimerization reactor considered in this study is assumed to be a liquid phase perfectly mixed reactor, i.e. no mass transfer limitation is considered in this system. Schematic of the process is depicted in Figure 1. The liquid is homogenized by a high re-circulation rate

around the reactor through a heat exchange used to remove the high exothermic heat of reaction. The model uses the Homo- and Co-polymerization mechanisms suggested by Galtier *et. al.* (1988). The reaction kinetics for the initiation, propagation and termination stages of the ethylene dimerization are given elsewhere (Ali and Alhumaizi, 2000).

Based on the above assumptions and the assumed reaction kinetics, the resulted dynamic model of the dimerization process is as follows (Ali and Alhumaizi, 2000):

$$V \frac{dC_4}{dt} = -Q\beta C_4 - V[(-b_2C_2 + a_4C_4 + b_4C_4)K_2 + a_4C_4K + b_4C_4K_4] \quad (1)$$

$$V \frac{dC_2}{dt} = FC_{2f} - Q\beta C_2 - V[a_2C_2(K + K_2 + K_4) + b_2C_2(K_2 + K_4 + K_6)] \quad (2)$$

$$V \frac{dK}{dt} = FK_f - Q\beta K - V[(a_2C_2 + a_4C_4)K + b_2C_2(K_2 + K_4 + K_6) + b_4C_4(K_2 + K_4)] \quad (3)$$

$$V\rho C_p \frac{dT}{dt} = F\rho_f C_{pf}(T_f - T_r) + Q(1-\beta)\rho C_p(T_R - T_r) - Q\rho C_p(T - T_r) + V(r_2(-\Delta H_1) + r_4(-\Delta H_2)) \quad (4)$$

$$V_c\rho C_p \frac{dT_R}{dt} = Q(1-\beta)\rho C_p(T - T_R) - UA(T_{Rav} - T_{cav}) \quad (5)$$

$$V \frac{dK_2}{dt} = -Q\beta K_2 + V[a_2C_2K - (a_2C_2 + a_4C_4 + b_2C_2 + b_4C_4)K_2] \quad (6)$$

$$V \frac{dK_4}{dt} = -Q\beta K_4 + V[a_2C_2K_2 - (a_2C_2 + b_2C_2 + b_4C_4)K_4 + a_4C_4K] \quad (7)$$

$$V \frac{dK_6}{dt} = -Q\beta K_6 + V[a_2C_2K_4 - b_2C_2K_6 + a_4C_4K_2] \quad (8)$$

where

$$T_{cav} = \frac{T_c + T_{co}}{2}$$

$$T_{Rav} = \frac{T + T_R}{2}$$

The dynamic of the outlet temperature of the coolant fluid is not included and alternatively it is obtained by solving the steady-state equation:

$$WCp_w(T_{co} - T_c) = U_h A_c (T_{Rav} - T_{cav}) \quad (9)$$

In this case,  $W$  (Coolant flow rate) and  $F$  (Gases feed flow rate) are used as forcing inputs. The kinetic parameters, i.e.,  $a_i$  and  $b_i$ , used in this study are based on the rate constants obtained by Galtier, *et. al.* (1988), and Woo *et. al.* (1991), and are given elsewhere (Ali and Alhumaizi, 2000). The definition of the process states and the various process parameters in the above equations is given in the nomenclature. Table 1 shows the numerical values of the design parameters for the dimerization reactor system. The original model of the dimerization process contains two additional states (Trabzoni, 1998). The two states, which represent the hexene and octene concentrations, are not included in this paper for simplicity. This assumption is valid since the above eight states are independent of the omitted ones.

It should be noted that, in the above model, arithmetic temperature average as driving force for heat transfer is used instead of log-mean temperature differences. The reason behind this treatment is to simplify the GLC scheme design. As will be shown later, the GLC design is based on solving the model equations for the design variable. Therefore, the solution becomes straight forward when the design variables appear linearly in the model equations.

### **Open-loop Analysis**

Our previous open-loop bifurcation analysis (Ali and Alhumaizi, 2000), revealed the existence of a trade-off between conversion and selectivity (yield), which is clear in Figure 2. It can be seen that as the feed flow rate  $F$  increases, the conversion increases while the yield decreases and vice versa. For this reason it is recommended to operate the plant around a favorable operating point that corresponds to  $F = 4 \times 10^{-3} \text{ m}^3/\text{s}$ , which corresponds to 95.7% conversion and 69.6% yield. This point also corresponds to a practical temperature operation, which has to be around the heavy mixture bubble point of 67 °C. Table 2 lists the process parameters at this favorable operating point. Nevertheless, as the open-loop response shown in Figure 3 indicates, the desired operating point is unstable. The stable regions for this process are economically unacceptable. For example, as shown in Figure 2 a stable region exists at high throughput, i.e., high  $F$ , but, in the same time, at low yield and selectivity. Another stable region is located at very low  $F$ , which corresponds to a high selectivity but low conversion and production rate. This region is not shown in the figure. Therefore, there is

a potential for utilizing a good control design to stabilize the reactor around the desired open-loop unstable point.

### **Control Objective**

The main control objective of such a process is the stabilization of the reactor temperature. This is essential to secure safe plant operation and to deliver a good quality product. It is also desirable to maintain optimal operation of high ethylene conversion and desired butene-1 yield as given in Table 2 in the face of plant upsets. In practice, the coolant feed temperature,  $T_c$ , is one possible source of disturbances to the process, which may cause thermal runaway due to temperature instability and consequently loss of conversion and/or yield. The upset in  $T_c$  is chosen for demonstration purposes and is considered to simulate an unknown unmeasured disturbance that creates a temperature excursion situation. For this reason, the closed-loop simulations in this paper focus on temperature stabilization and maintaining desired yield in the face of upsets in  $T_c$ . In this case, the controlled variable would be the reactor temperature, ( $T$ ), and the butene concentration at the outlet stream, ( $C_4$ ). In due course, the suitable manipulated variables (MV) are the coolant flow rate,  $W$ , and the feed flow rate  $F$ . Single-input single-output (SISO), multi-input single output (MISO) and MIMO control schemes will be examined for this control problem. For the SISO case, the controlled variable is the reactor temperature and the manipulated variable is the coolant flow rate. The MIMO scheme is carried out in a decentralized form where  $T$  is regulated via  $W$  and  $C_4$  via  $F$ . In the MISO scheme, the two manipulated variables, i.e.,  $W$  and  $F$ , will be driven by the same error signal, which is the deviation of  $T$  from its set point. The selection of these particular manipulated variables and their pairing procedure are based on our earlier work (Ali and Alhumaizi, 2000) which includes detailed analysis for designing the control structure of the dimerization reactor. In the simulation section, a sampling rate of 0.1 hr will be used, which is more realistic for practical applications.

### **Fuzzy Logic Control Algorithm**

The basic FLC loop is shown in Figure 4. It consists of three major sequential steps, namely Fuzzification, Inference engine and Defuzzification. In the following subsections, the development and design of each step is discussed in detail. Hereafter, by input we mean controller input, i.e. error and/or error velocity signal and by output we mean the controller output, i.e. manipulated variable.

*Fuzzification:*

The input signal of the controller, which is a real-value variable also known as crisp value, is fed to the fuzzifier. In the fuzzifier, the crisp value is converted as a member of a finite number of fuzzy sets. Therefore, the process of fuzzification is simply mapping, i.e. checking the value of the input signal (member) against each fuzzy set to determine its degree of membership (belongingness). The fuzzy set is usually represented as a membership function as shown in figure 5. The membership function can have any symmetrical geometric shape and is graded between 0 and 1. The fuzzy sets in Figure 5 are identified by linguistic names such as Large Positive (LP), Small Positive (SP), Zero (ZE), Small Negative (SN), Large Negative (LN) and they are labeled as  $\mu_1$ ,  $\mu_2$ ,  $\mu_3$ ,  $\mu_4$  and  $\mu_5$ , respectively. Usually, finite number of overlapping membership functions (fuzzy sets) can be used to span the possible range of the process variable. The overall span (domain of a specific variable) is known as the universe of discourse.

Common difficulties exist in this step. The selection of the shape and number of the membership functions, the location of their center, i.e. where the fuzzy set has a maximum value, and the size of the universe of discourse is not straight forward. Moreover, the common FLC design involves at least three different groups of fuzzy sets, each of which corresponds, to a different process variable. For example one group is used for the error signal,  $e$ , another for the velocity of error signal,  $\Delta e$ , and another for the controller's output (manipulated variable),  $u$ . The latter is used in the defuzzification step. In this paper we try to overcome the above problems. First we use only one group of fuzzy sets for all the three process variables. To achieve this, the universe of discourse is unified so that it spans the interval  $[-1, +1]$ . In this case, the value of each process variable should be scaled properly to fit the specific interval. This idea of normalizing the fuzzy set domain is proposed by Qin and Borders, 1994. Discussion of the scaling procedure is given under the tuning section. Secondly, Gaussian and sigmoidal shapes are considered for the membership functions. Gaussian shape is selected because it is a continuous function and can be easily expressed by an analytical formula. Continuity of the Gaussian functions produces smoother control output. Usually to symmetrically span the input domain, odd number of fuzzy sets should be designed. Increasing the numbers of the fuzzy sets creates smoother output. However, this

will be at the expense of increasing the number of control rules leading to more complicated design procedure and tuning. Therefore, five such functions are used here as shown in Figure 5, which found, with the aid of Gaussian functions, sufficient to provide smooth output at reasonable number of fuzzy rules.

In this work, two variables are fuzzified, which are the error ( $e$ ) and the error velocity ( $\Delta e$ ). Therefore, in this controller phase, the membership degree of a specific input value, i.e.  $e$  or  $\Delta e$ , over all fuzzy sets can be determined directly from Figure 5.

#### *Inference Engine:*

Inference engine is the heart of the FLC algorithm where the control action is formulated. Specifically, it describes the output of the controller for all input signals combination. It consists of several fuzzy set rules represented by conditional statements in the form of IF-Then rules as shown in Table 3 (Yen and Langari, 1999). The collection of all rules is called Rule Base. Generation of such rules is another difficult part of the FLC design.

In this paper, we choose to design the rule base according to desired response of the process because it the most intuitive for many control practitioners. The rule base for a generic feedback response as listed in Table 3 is used here. Note that the AND command is a common fuzzy rule operation, which mathematically implies the minimum of two values. Note that the first index of  $\mu$  is the label for the membership function. The second index indicates the rule number.

At this phase of the controller algorithm, given a value for the input signal, the degree of fulfillment of each rule in the rule base set is determined. The degree of fulfillment of the rule base is known as the conclusion or the result of the rule base. The process in which these conclusions are calculated is known as inference. Due to overlapping membership functions, some of the rule conclusions may have a zero value and some a non-zero value. Membership function for the output with a non-zero degree of fulfillment is considered fired. In standard FLC algorithms, the fired functions are clipped or scaled and then copied to a temporary template. All fired sets are then combined using superimposing technique. The combined set is known as the inferred controller output. Figure 6 shows an example of three combined active fuzzy sets.

*Defuzzification:*

In this step, the combined output fuzzy sets (inferred output from the previous step) are then converted (defuzzified) into a single crisp value. The calculated crisp value is the numerical value for the manipulated variable. Defuzzification is thus equivalent to finding the weighted average value for the combined sets. In standard FLC applications, the combined set is a new geometric shape, say  $\mu_{out}$  (Figure 6). Hence, finding a weighted average is similar to determining the geometric center. One way is by calculating the center of area (COA) (Yen and Langari, 1999). The discretized form of COA can be written as:

$$\Delta u = \frac{\sum_{j=1}^{n_R} \sum_{i=1}^{n_f} \mu_{j,i} \delta_i A_{j,i}}{\sum_{j=1}^{n_R} \sum_{i=1}^{n_f} \mu_{j,i} A_{j,i}} \quad (10)$$

Where  $n_f$  is the number of output membership functions and equals 5 in this paper,  $n_R$  is the number of rules and equals 25 in this paper, which is the maximum possible number to cover all eventualities created by the 5 output membership functions.  $\delta_i$  is value for the location of the center of  $\mu_i$ . The value of  $\delta_i$  is pre-calculated and fixed as shown in figure 5.  $A$  is  $n_R \times n_f$  pre-calculated matrix, which identifies which membership function is included in each Rule. For example, row 1 of matrix  $A$ , which is assigned for Rule 1, contains 1 at the first column and zeros elsewhere. The same logic is carried out over the remaining rows.

It should be emphasized that the control output,  $\Delta u$  computed by Eq. 10 is taken in the velocity form. Velocity form is more suitable for non-linear systems. In non-linear systems, the new equilibrium value for  $u$ , denoted as  $u_{ss}$ , that brings the output to the desired steady state value may not be known beforehand. Thus, it is difficult to locate  $u_{ss}$  in the universe of discourse as the center for the ZE membership function. However, when  $\Delta u$  is used, zero value will always be the equilibrium point around which ZE can be built.

*Tuning method:*

Tuning a fuzzy linguistic controller to changing process and environment dynamics can be accomplished in several different ways:

- Adjusting the membership functions.
- Changing the finite set of values describing the universe of discourse.
- Reformulating the finite set of control rules in the knowledge base (inference engine).

However, these procedures are cumbersome. In addition, there are no clear guidelines on how these procedures affect the closed-loop response. In this paper, we adopt a simpler method. The scaling factors for the input and output signals are used as the tuning parameters. As will be seen in the examples, these factors have direct and clear effect on the closed-loop response. These factors are used to scale the process variables so that they fit the universe of discourse domain used in Figure 5. Specifically, the scaling factors for the error, error velocity, and output velocity are  $se = a/sp$ ,  $sde = b/sp$  and  $sdu = c\Delta u_m$  respectively. For servo control problems,  $sp$  is the difference between the set point and the initial steady state value for the controlled variable. For regulatory control problem,  $sp$  is the set point value.  $\Delta u_m$  is the difference between the maximum and minimum allowable values for the manipulated variable. Therefore,  $a$ ,  $b$ , and  $c$  are the tuning parameters. Changing the value of  $a$ ,  $b$ , or  $c$  is equivalent to stretching or expanding the universe of discourse of the fuzzy sets shown in Figure 5. Conceptually, this is similar to the first two tuning guidelines mentioned above.

*FLC algorithm:*

The following steps explain the FLC control algorithm used in this paper.

Set  $a=b=c=1$ . At any sampling time,  $k$  do:

**Step1:** scale the error and the error velocity signals ( $e(k)$ ,  $\Delta e(k)$ ) via multiplying them with  $se$  and  $sde$ .

**Step2:** Compute the degree of membership of  $e(k)$  and  $\Delta e(k)$  to the five membership functions shown in Figure 5.

**Step3:** Calculate the conclusions of the Rule base as given in Table 3.

**Step4:** Calculate the control action using equation 10. Scale the computed value by multiplying with  $sdu$ .

**Step 5:** Implement the control action, set  $k=k+1$  and go back to step 1

If the control performance is poor, adjust the value of  $a$ ,  $b$ , or  $c$ . We have found that increasing the value of  $a$  increases the speed of response and eliminates offset. Increasing the value of  $c$  penalizes the manipulated variable moves, thus introduces stabilizing effect.

The main advantage of FLC, besides being a nonlinear controller, is its independence on process model as the latter is expensive or difficult to obtain. The drawback of such algorithm arises from the complexity of designing the fuzzy sets and the fuzzy rules. This is because these sets and rules are usually built based on heuristic and engineering knowledge.

### **Globally Linearizing Control Algorithm**

This approach uses an explicit process model usually in the form of state space to derive analytical nonlinear control law. Geometric theory, specifically Lie derivatives, is used to determine the relative order of the process model (Kravaris and Kantor, 1990). The relative order is basically the number of times that the output must be differentiated till the manipulated variable appears explicitly in the observed state equation. The obtained equation is then solved for the manipulated variable such that the closed-loop response tracks a certain desired closed-loop behavior. The desired trajectory must possess an order equals to or greater than the relative order.

#### *SISO control scheme*

The manipulated variable ( $W$ ) does not appear explicitly in the state equation for  $T$ , i.e. equation (4). In due course, the differential equation for  $T$  can be differentiated once generating a second order differential equation for  $T$ . The ordinary differential equation (ODE) for  $T_R$  (Equation (5)) can then be inserted into the resulted second-order ODE in order to incorporate  $W$  explicitly into the equation. The process in this case is said to have a relative order of two. Consequently, a second or higher order reference trajectory should be designed for the output. Alternatively, the relative order can be reduced to one and thus, a first order reference trajectory can be sufficient. This can be achieved by writing the overall energy balance:

$$V\rho C_p \frac{dT}{dt} = F\rho_f C_{pf}(T_f - T_r) - WC_{pw}(T_{co} - T_c) - F\rho C_p(T - T_r) + VR_H \quad (11)$$

where  $R_H = r_2(-\Delta H_1) + r_4(-\Delta H_2)$ . Solving the above equation for the manipulated variable ( $W$ ) gives:

$$W = \frac{1}{C_{pw}(T_{co} - T_c)} \left[ -V\rho C_p \dot{T} + F(\rho_f C_{pf}(T_f - T_r) - \rho C_p(T - T_r)) + VR_H \right] \quad (12)$$

Hence, a second order reference trajectory for the output can be selected as:

$$\dot{T} = \tau_1(T^{sp} - T) + k_{i1} \int_0^t (T^{sp} - T) dt \quad (13)$$

Here  $\tau_1$  and  $k_{i1}$  are tuning parameters. The integral action is incorporated to eliminate steady state offset. Equation (12) and equation (13) comprise the SISO GLC control law for the temperature loop.

*MIMO control structure:*

Beside the above control loop, there will be another loop relating  $C_4$  with  $F$ . Clearly  $F$  appears explicitly in equation (1) and equation (4). However,  $W$  appears only in the overall energy balance equation. Thus, the 2x2 system is partially decoupled. Assuming total decoupling, and noting that  $F = Q\beta$ , equation (1) can be solved for  $F$  giving:

$$F = -\left[ \dot{C}_4 + (-b_2 C_2 + a_4 C_4 + b_4 C_4) K_2 + a_4 C_4 K + b_4 C_4 K_4 \right] V / C_4 \quad (14)$$

Since the second loop has a relative order of one, a second order reference trajectory for the second output can be used as follows:

$$\dot{C}_4 = \tau_2(C_4^{sp} - C_4) + k_{i2} \int_0^t (C_4^{sp} - C_4) dt \quad (15)$$

Equation (14) and (15) comprise the GLC law for the second loop.  $\tau_2$  and  $k_{i2}$  are the corresponding adjustable parameters. When the MIMO structure is employed in total decoupling fashion, equations 12 to 15 are solved independently, i.e.  $F$  is fixed in equation (12).

On the other hand, when the MIMO scheme is employed in partial de-coupling fashion, equation (14) and (15) are solved first and then the resulted value for  $F$  is substituted in equation (12).

*MISO control structure:*

The MISO scheme consist of one controlled output, which is the reactor temperature ( $T$ ) and two manipulated variables namely; the feed flow rate  $F$  and the cooling flow rate  $W$ . Apparently, both manipulated variables appear explicitly in the overall energy balance [equation (11)]. The latter can be written as follows:

$$V\rho C_p \dot{T} - VR_H = F\alpha_1 + W\alpha_2 \quad (16)$$

Because the above equation has two unknowns, one possible solution is the least squares solution:

$$F = \frac{\alpha_1}{\alpha_1^2 + \alpha_2^2} V[\rho C_p \dot{T} - R_H] \quad (17)$$

$$W = \frac{\alpha_2}{\alpha_1^2 + \alpha_2^2} V[\rho C_p \dot{T} - R_H] \quad (18)$$

Equation (17) and (18) along with equation (13) comprise the MISO control law. This control scheme has only one set of tuning parameters, i.e.  $\tau_1$  and  $k_{il}$ . However, since the two variables are of different order of magnitude, a proper scaling should be used. Consequently,  $\alpha_1$  and  $\alpha_2$  are scaled through pre-multiplied them by the corresponding maximum value of  $F$  and  $W$  respectively. Therefore, before implementing the value of  $F$  and  $W$  calculated from equation (17) and (18), they should be re-multiplied by the scaling factor to retrieve their raw values. The MISO control scheme based on the least-squares solution does not necessarily provide the best dynamic response however; it is simply an intuitive attempt to improve the feedback performance.

The GLC scheme is illustrated via the block diagram shown in Figure 7. In this paper, we consider practical implementation schemes. We consider that the plant states are partially measured. Therefore, a parallel model observer should be used to estimate the other

unmeasured plant states as shown in figure 7. In this case, the feedback signal is the difference between the plant measurement and the model output. In addition, the model states that represent the unmeasured plant states are fed to the nonlinear controller. Moreover, the control law (Eqns 12-18) represented by the block called “nonlinear control” contains several unmeasured model parameters. Consequently, the effect of some degree of uncertainty in these parameters should be also investigated. It should be noted that the above control laws are implemented in a discrete-time formulation, thus, the integral is approximated numerically by summation.

Robustness of the GLC algorithm is addressed here through simple feedback compensation (Hu and Rangaiah, 1999). Generally, the GLC algorithm, like other model-based algorithms, performs well when the model is perfect. However, the performance may degrade substantially or even becomes unstable in the presence of model uncertainty. This situation lead the researcher to incorporate parameters and state estimation techniques (Tracy and McGregor, 1997; Assala et. al., 1997; and Soroush, 1997). However, this issue is out of the scope of this paper. Alternatively, simple state resetting through standard disturbance (or model-plant mismatch) estimation is used. This simple treatment is found sufficient. The model states are reset every sampling time by adding to them the following estimate of model-plant mismatch:

$$D_i(k) = y_{pi}(k) - y_{mi}(k), i = 1, ny \quad (19)$$

Where  $k$  is the sampling instant, and  $ny$  is the number of outputs.  $y_p$  denotes the measured output and  $y_m$  is the corresponding model output. In practice,  $y_p$  is obtained from plant measurement, however, in this paper it is obtained from numerical integration of the process model. Similarly,  $y_m$  is obtained from the numerical integration of the process model. The process model is the set of ODE's (Equation 1-8). In order to simulate model-plant mismatch, some of the model parameters have different values when used to obtain  $y_p$  than when used to obtain  $y_m$ . The difference in these values will be discussed in the next section when GLC implementation is discussed.

The advantage of GLC methods is the ability to deliver perfect control and globally stable response if the model is perfect. The disadvantages include the requirement of a

special model form such as state space equations. In this case all model parameters and states appear in the control law. Therefore, robustness is an important issue especially in the presence of errors in the model parameters and states.

### **Non-linear MPC algorithm**

In this paper the structure of the MPC version developed by Ali and Zafiriou (1993) that utilizes directly the nonlinear model for output prediction is used. A usual MPC formulation solves the following on-line optimization:

$$\min_{\Delta u(t_k), \dots, \Delta u(t_{k+M-1})} \sum_{i=1}^P \left\| \Gamma(y(t_{k+i}) - R(t_{k+i})) \right\|^2 + \sum_{i=1}^M \left\| \Lambda u(t_{k+i-1}) \right\|^2 \quad (20)$$

subject to

$$C^T \Delta U(t_k) \leq B \quad (21)$$

For nonlinear MPC the predicted output,  $y$  over the prediction horizon  $P$  is obtained by the numerical integration of:

$$\frac{dx}{dt} = f(x, u, t) \quad (22)$$

$$y = g(x) \quad (23)$$

from  $t_k$  up to  $t_{k+P}$  where  $x$  and  $y$  represent the states and the output of the model respectively. The symbols  $\| \cdot \|$  denotes the Euclidean norm,  $k$  is the sampling instant,  $\Gamma$  and  $\Lambda$  are diagonal weight matrices and  $R$  is the desired output trajectory.  $\Delta U(t_k) = [\Delta u(t_k) \dots \Delta u(t_{k+M-1})]^T$  is a vector of  $M$  future changes of the manipulated variable vector  $u$  that are to be determined by the on-line optimization. The control horizon ( $M$ ) and the prediction horizon ( $P$ ) are used to adjust the speed of the response and hence to stabilize the feedback behavior.  $\Gamma$  is usually used for trade-off between different controlled outputs.  $\Lambda$ , on the other hand, is used to penalize different inputs and thus to stabilize the feedback response.

The usual implementation of MPC involves numerical integration of the model state equations over the prediction horizon  $P$  to obtain the future output behavior. Then, the objective function (Eq. 20) is solved on-line to determine the optimum value of  $\Delta U(k)$ . Only the current value of  $\Delta u$ , which is the first element of  $\Delta U(k)$ , is implemented on the plant. At the next sampling instant, the whole procedure is repeated. There are two methods of solution of the NLMPC optimization problems. The sequential solution iteratively solves the ODE's as an inner loop to evaluate the objective function. The simultaneous solution transforms the ODEs to algebraic equations which are solved as nonlinear equality constraints. The first approach is adopted here. It should be noted that NLMPC is not restricted to a special type of nonlinear models. Black box models can also be used.

A disturbance estimate (or model-plant mismatch), as defined by equation (19), should also be added to  $y$  in Equation (23) or alternatively it can be absorbed in  $R(t_{k+1})$ . In the standard MPC implementation, the disturbance is assumed constant over the prediction horizon, and is set equal to the difference between plant and model outputs at present time,  $k$ . The function of the "additive" constant disturbance in the model prediction is to introduce integral action and thus removes steady state offset in the presence of model uncertainty or unmeasured disturbances. For unstable processes, improving the model prediction by the additive constant disturbance is not enough solely. In fact, state estimator and/or parameter estimation should be used in conjunction with the additive corrections.

The original NLMPC algorithm (Ali and Zafiriou, 1993) is equipped with Kalman filtering to improve the controller performance for open-loop unstable processes. Kalman filtering requires repeated solution of Riccati differential equations, which may not converge if the original nonlinear model is highly unstable (Ali and Elnashaie, 1997). Alternatively, the Kalman filter gain is estimated by solving a small-size optimization problem (Ali and Elnashaie, 1997). However, like other state observers, the proposed observer is stable only for bounded input. In this particular application, the input to the proposed state estimator (modified Kalman Filter), which is the model-plant mismatch, is sometimes unbounded. This situation leads to unsatisfactory application of the proposed state observer. As intuitive remedy, the model states are updated by simply adding to them, the estimate of model-plant mismatch (Equation 19). This is exactly the same procedure used in the GLC algorithm. It

should be noted that this is done in addition to the output correction mentioned in the beginning of the previous paragraph.

In addition to the general features of the MPC mentioned in the introduction section, NLMPC is more suitable for highly nonlinear processes. The main drawback of such a scheme is the computational effort and time needed to solve the optimization problem. The performance and stability of the algorithm depends on good tuning. Robustness in the face of modeling errors can be improved by incorporating state and/or parameter estimation techniques.

### **Closed-loop simulations**

#### *PI controller*

The results in this section are adopted from our earlier work (Ali and Alhumaizi, 2000). It is reproduced here for comparison purposes. The PI setting values are determined by continuous cycling method as reported in (Ali and Alhumaizi, 2000). Simulation of the SISO control problem for +4°C and +6 °C step changes in  $T_c$  using the PI control is shown in Figure 8. As shown in the figure, for +4°C upset the reactor temperature is well maintained at its set point. It is obvious that by regulating the reactor temperature, the reaction yield, represented by the  $C_4$  response, is also kept at the desired favorable set points of 69.6%. The PI settings for this case are  $k_c = -1000 \text{ kg/s.}^\circ\text{C}$  and  $\tau_I = 10 \text{ ks}$ . However, at an upset of magnitude of +6 °C in  $T_c$ , more amount of coolant is needed to remove the heat of reaction leading to saturation of the coolant flow rate. This degrades the closed-loop performance. A loss in the yield is also observed. The PI controller gain in this case is the same as before, however the integral time ( $\tau_I$ ) is re-tuned for stability by trial-and-error to 100 ks.

Another way to deal with the case of rejecting +6 °C change in  $T_c$  is to use a MIMO control structure. The solid lines in Figure 9 illustrate the effect of employing the MIMO control scheme to handle such challenging problem. The corresponding PI settings are  $k_c = [-1000 \text{ kg/s.}^\circ\text{C}, -5 \times 10^{-7} \text{ (m}^3\text{/s)/(mole/m}^3\text{)}]$  and  $\tau_I = [2000 \text{ s}, 0 \text{ s}]$ . In this case, the MIMO scheme managed to perfectly regulate the first controlled variable,  $T$  while the second controlled variable  $C_4$ , suffers from an offset of -73 mole/m<sup>3</sup>. Our investigations observed that any attempt to reduce the offset would create persistent oscillatory response for the reactor temperature. Moreover, tuning of the MIMO scheme is difficult due to the strong

interaction behavior. In fact, the disturbance causes the reactor temperature to increase rapidly. As a result the first control loop will increase  $W$  till it brings the temperature back. During the temperature excursion, the reaction activity diminishes causing sharp drop in the yield. The latter causes the second control loop to reduce the feed rate in order to recover the yield. However, because  $C_4$  has very slow dynamic compared to the reactor temperature, it takes longer time for the yield to recover. If the settings of the second loop are tuned to produce faster response, then adverse effect will be introduced in the first loop. This will cause undesirable behavior in the temperature loop as mentioned earlier.

Alternatively a MISO PI scheme can be used. In due course, the temperature will be controlled by both  $W$  and  $F$  simultaneously in a split range mode. It should be noted that 90% of the error signal will be used to actuate  $W$  and the rest to actuate  $F$ . The split range ratio is used only in the PI controller and is chosen mainly to avoid over utilization of both MVs and secondly to give more weight to the coolant flow. Tuning will be easier because interaction is not involved. In addition, the higher degree of freedom can help to perfectly control the reactor temperature. This will also bring the response of  $C_4$  to the corresponding steady state value (desired set point). This is evident from the dashed lines shown in Figure 9. Obviously, less overshoot in the reactor temperature response and less offset ( $-26 \text{ mole/m}^3$ ) in the yield response are observed. In fact, since both  $W$  and  $F$  are used to regulate the reactor temperature, they managed to minimize the temperature overshoot. This in turn minimized the reduction in yield. The PI settings used are  $k_c = [-1000 \text{ kg/s.}^\circ\text{C}, 0.002 \text{ m}^3/\text{s.}^\circ\text{C}]$  and  $\tau_i = [100 \text{ ks}, 50 \text{ ks}]$ .

### *Fuzzy Logic Controller*

The above SISO, MISO and MIMO control problems are re-tested using the FLC algorithm. Regarding the SISO case, Figure 10 demonstrates the closed loop response to two step changes in  $T_c$  of  $+4$  and  $+6$   $^\circ\text{C}$ , respectively. For both cases,  $a = 1$ ,  $b = 10$  and  $c = 10^5$  are used. As the figure illustrates, a perfect disturbance rejection without offset is obtained for the first case, i.e.  $\Delta T_c = +4$   $^\circ\text{C}$ . For the larger disturbance case, i.e.,  $\Delta T_c = +6$   $^\circ\text{C}$ , poor performance, which seems worse than that for the PI algorithm, is obtained. The poor temperature control is associated with a loss in the yield, which is not shown in figure 10 for simplicity. The SISO FLC performance can be made less aggressive through tuning. However, the closed-loop response will eventually oscillate due to input saturation. The SISO PI response also oscillates if aggressive values for the tuning parameters are used or if longer

simulation time is used in Figure 8. Anyhow, further improvement in the FLC performance is not possible in this case because the loss in performance is due to input constraints.

Building upon the poor performance faced in the SISO case at large upset in the inlet cooler temperature, a MIMO FLC scheme is examined. In this case, a decentralized control system similar to that used in the PI algorithm is also used here. The result of the closed loop response is shown in Figure 11 by the solid lines. For the first loop,  $a = 1$ ,  $b = 100$ , and  $c = 10^5$  are used, while  $a = 1$ ,  $b = 3 \times 10^3$  and  $c = 1 \times 10^{-5}$  are used for the second loop. Tuning is found to be a cumbersome task due to the strong cross interaction. Nevertheless, the obtained closed loop response is reasonable as perfect control of  $T$  and minor offset in  $C_4$  (-67 mole/m<sup>3</sup>) are observed. Small reduction in the feed flow rate was necessary to reduce offset in the yield, but was not good enough. Further tuning was found not helpful. On the other hand implementation of the MISO control structure provided excellent offset-free response as shown in Figure 11 by the dashed line. The FLC tuning parameters are the same as in the MIMO case except that  $c$  for the second loop is re-adjusted to  $1 \times 10^{-4}$ . The only reported advantage of the FLC is that its resulted performance for the MISO case outperforms that obtained by the PI algorithm. However, the MISO FLC is superior to the MIMO FLC in the sense of less offset in the yield response. This situation is attributed to the strong cross-loop interaction. In the MIMO case, tuning the second control loop to reduce offset in the yield would require less fresh feed flow. Alteration of the fresh feed flow introduces disturbance to the first control loop leading to temperature runaway and consequently unstable process behavior. Moreover, it is found that tuning the FLC parameters for the MIMO case is as difficult as that for the MIMO PI algorithm.

#### *Globally linearizing controller*

The GLC algorithm is also tested for the same control objective in SISO, MIMO and MISO modes. In the following applications, the reactor temperature and the butene concentration states are assumed measured, while the rest are unmeasured. Therefore, in the GLC control law (Eqns 12-18), the plant states are used for the measured states and the model states for the unmeasured ones. The values of the model states are obtained by direct integration of the process model equations. The values of the plants states are supposed to be obtained from the plant measurement, however in this paper they are obtained from integration of the process plant equations. The latter is exactly the same as the model

equation except in two aspects. First, the values of the process parameter values may differ as indicated later. Second, the upsets in the cooler inlet temperature affect only the plant equations but not the model equations. This procedure reflects the actual application in practice. Therefore, in all the following simulations the reaction rate constant  $a_2$  and  $a_4$  of the model are assumed 30% less than those of the plant. The overall heat transfer coefficient ( $U$ ) of the model is assumed 20% higher than that of the plant. The measured states are  $T$  and  $C_4$  while the unmeasured states are the catalyst concentrations, i.e.  $K$ ,  $K_2$ ,  $K_4$  and  $K_6$ . Note that all aforementioned states are utilized in the GLC control law. The idea of incorporating parametric errors and unmeasured states is to introduce model-plant mismatch and hence test the robustness of the GLC algorithm. For this reason, the standard disturbance estimation, i.e. model states resetting, proposed earlier is incorporated in the control algorithm.

Figure 12 shows the closed loop response for  $\Delta T_c = +4$  °C using the SISO GLC algorithm. The GLC parameters are  $\tau = 1$  s<sup>-1</sup> and  $k_i = 0.01$  s<sup>-2</sup>. As figure 12 demonstrates, GLC was able to stabilize the reactor temperature in that case and consequently to maintain a proper butene yield. However, at  $\Delta T_c = +6$  °C, the reactor temperature suffers from higher overshoot and steady state offset. As a result, a loss of butene yield is observed (Fig. 12). The reason for temperature offset is input saturation. Although, the coolant flow rate is not completely saturated, any attempt to remove the offset through controller tuning results in excessive oscillation. It should be noted that the adjustable parameter  $k_i$  is re-tuned for the last case to  $5 \times 10^{-4}$  s<sup>-2</sup> to preserve stability. It is worth to mention that the GLC performance without model state resetting is not shown here for simplicity. The reason for exclusion is that the feedback response without state resetting does not differ than those shown in figure 12 except of minute periodic spikes produced by the effect of parametric modeling errors.

To overcome the loss of controllability in the SISO case, a MIMO GLC scheme is examined for the  $\Delta T_c = +6$  °C case. Figure 13 depicts the result for this case. The values for the GLC tuning parameters are  $\tau_1 = 1$  s<sup>-1</sup>,  $k_{i1} = 5 \times 10^{-4}$  s<sup>-2</sup>,  $\tau_2 = 10^{-4}$  s<sup>-1</sup> and  $k_{i2} = 0$  s<sup>-2</sup>. As figure 13 shows, with the model state resetting is incorporated in the GLC law, very successful closed loop response for both  $T$  and  $C_4$  is obtained. The second control law is only implemented after twice the process time constant, i.e., 10 hrs, has elapsed. This is to ensure that the reactor temperature has been stabilized. If the second control law is implemented at zero time, poor performance will result due to strong interaction. It should be noted that the

response of both  $T$  and  $C_4$  suffer from slight offset of  $0.1\text{ }^\circ\text{C}$  and  $-74\text{ mole/m}^3$ , respectively. Our simulation revealed the existence of trade off between the performances of the two loops. When  $\tau_1$  is tuned to eliminate the offset in  $T$ , steady state noise is produced in butene ( $C_4$ ) response. On the other hand, when  $\tau_2$  is tuned to eliminate offset in  $C_4$ , larger offset is produced in  $T$  response.

As expected, implementation of the MISO control scheme delivered improved performance compared to that obtained using the MIMO scheme as shown by the dashed lines in Figure 13. The offset in  $C_4$  is further reduced to  $-7\text{ mole/m}^3$ . The GLC parameters are  $\tau = 1\text{ s}^{-1}$  and  $k_i = 1 \times 10^{-4}\text{ s}^{-2}$ . Note that both control loops are activated at zero time, i.e. no time delay is introduced in the second loop as in the MIMO case. Overall, the GLC algorithm illustrated some merit over the PI algorithm, but at the expense of additional effort associated with designing the GLC algorithm. Note that the GLC algorithm requires developing and utilizing a process model.

#### *NLMPC controller:*

In all the following simulations, the same model parameter alterations employed in the GLC controller is also considered here. The purpose is to test the robustness of the model-based controllers in the presence of modeling errors. The NLMPC performance is tuned by trial and error according to general guidelines. In general, increasing  $P$  improves stability and robustness of the response. Increasing  $\lambda$  penalizes the corresponding input moves creating slower and more stable response. The weighting matrix  $\Gamma$ , is used primarily for scaling in the multivariable case; it permits the assignment of more or less weight to the objective of reducing the predicted error for the individual output variables.

The solid line of Figure 14 demonstrates the response of the dimerization process to step change of  $+4^\circ\text{C}$  in  $T_c$  using SISO NLMPC algorithm. Note the model state  $T$  is re-set using the estimated modeling error (Eqn 19) as discussed earlier. The tuning parameter values for this case are  $M = 1$ ,  $P = 11$  and  $\lambda = 0.008$ . As expected, perfect rejection of the effect of the disturbances is obtained. However, at an upset of  $+6^\circ\text{C}$  in  $T_c$ , the closed-loop response for the reactor temperature suffers from a temperature offset due to the effect of input saturation as shown in Figure 14 by the dashed line. This situation created a larger

steady state offset for the yield. The tuning parameter values for this case are  $M = 1$ ,  $P = 15$  and  $\lambda = 0$ . Further performance improvement through controller tuning is found useless.

The dashed line in Figure 15 shows the feedback response for an upset of  $+6^\circ\text{C}$  in  $T_c$  using NLMPC with MISO scheme. The tuning parameters are  $M = 1$ ,  $P = 20$ ,  $\Lambda = \text{diag}[0,10]$ . Like the other algorithms, improved closed-loop response is observed. Specifically  $-9 \text{ mole/m}^3$  offset in  $C_4$  is obtained. The solid line in Figure 15 illustrates the feedback response for an upset of  $+6^\circ\text{C}$  in  $T_c$  using NLMPC with MIMO scheme. The tuning parameters for this case are  $M = 1$ ,  $P = 22$ ,  $\Lambda = \text{diag}[0,10]$  and  $\Gamma = \text{diag}[1,0.01]$ . Interestingly, unlike the other algorithms the NLMPC response in the MIMO case outperforms that of the MISO case in the sense of less offset in  $C_4$  ( $-4 \text{ mole/m}^3$ ). In addition, the reactor temperature response had the lowest overshoot over all other algorithms. Inferiority of the MIMO scheme of the other control algorithms is attributed to the fact that they operate in a decentralized structure. Therefore, the function of the additional control loop, more specifically the additional degree of freedom,  $F$ , is devoted for regulating the butene concentration only. Perfect control of the additional loop may not be satisfied unless the reactor temperature is well stabilized and is offset free. The MIMO structure in the NLMPC algorithm operates in a fully multivariable fashion, which is one of the advantages of such an algorithm. With special adjustment of the output weights,  $\Gamma$ , more weight can be given to the most important variable, i.e. the reactor temperature in this case. However, we should admit here that tuning the MIMO NLMPC is a difficult task due to the internal instability augmented with the strong cross-loop interaction. Careful procedure should be used when fine-tuning the NLMPC. Large changes in the tuning parameters create unsatisfactory performances and unpredictable effect on the response. This behavior does not provide a meaningful guideline on how to further fine-tune the feedback performance. Our experience in this problem indicates that stepwise and infinitesimal changes should be adopted for fine tuning the NLMPC especially in the MIMO case.

It can be argued that a better state estimation or disturbance prediction technique is required to enhance the NLMPC feedback performance. Our simulations revealed that the performance can not be improved even when the disturbance is treated as fully measured and that no parametric errors exist. By fully measured disturbance we mean that the upset in  $T_c$  affects both the model and plant, this is also known as feed-forward compensation. In this

case, the NLMPC performance with feed-forward and without modeling errors should outperform that with any optimal state or disturbance estimator. This is because simulation using feed-forward and perfect model makes the model states exactly equal the plant states.

*Overall analysis:*

Table 4 summarizes some performance criteria for the four tested control algorithms. The selected performance criteria are the offset in yield presented by the absolute deviation of steady state butene concentration from its set point, the overshoot in reactor temperature presented by the maximum value achieved during simulation and the settling time for the reactor temperature. The settling time is defined as the first time at which the temperature response reaches its final static value. The offset in the reactor temperature is not included in the comparison because the offset in  $C_4$ /yield is considered more important. According to the results reported in table 4, the SISO structure has the worst performance for all control algorithms and that the MISO structure has the best performance for all cases except for NLMPC. For the latter, the MIMO structure delivered the best performance over all control strategies and implementation schemes. However, some other practical comparison issues might be considered. For example, the PI and FLC algorithms do not require a process model. Tuning of the PI and the NLMPC are somewhat difficult especially for the MIMO case.

In all the simulations shown previously, offset was observed in the  $C_4$  response. However, this is not attributed to poor design or to improper handling of modeling error because some the strategies are model free. In the model-based controllers, perfect models were tested, but offset was still observed. Therefore, possible explanation of the poor performance in some cases is the difficulty of the control problem and tuning. Generally, perfect control of the reactor temperature is essential to stabilize the reactor and to maintain the yield because the latter is strongly affected by the temperature. The coolant flow,  $W$  affects the temperature directly and the yield indirectly through the temperature. In the model used here, the catalyst feed flow is related to the total feed flow,  $F$ . Therefore, the total feed has dual effect and cross-loop interaction. Dual effect means that  $F$  has simultaneous positive and negative effect on the reactor temperature. Cross interaction means that  $F$  has opposite

effect on the reactor temperature and on the yield. For example, increasing  $F$  will help in reducing the temperature because the gas flow acts like a cooling medium. In the same time, the increase in  $F$  will propagate the catalyst flow leading to a higher reaction activity. This situation will escalate the temperature. Note also that increasing  $F$  will decrease the yield. Decreasing  $F$  will create exactly the opposite effect. It should be noted though, that the thermal effect of  $F$  due to reaction activity is more dominant than that due to heat transfer.

According to the strong interaction discussed above, it is difficult to maintain the MIMO control objective unless a fully-coupled multivariable controller is used. This explains the superiority of NLMPC in this case. However, some offset in the yield was still observed in the MIMO NLMPC. This is because tuning was extremely difficult due to internal instability as mentioned earlier. On the other hand, one would expect the MISO scheme to control  $T$  perfectly because the cross-loop interaction does not exist. This was found true for all cases. However, offset-free response for the yield is not guaranteed because its control loop is open. Therefore, the resulted  $C_4$  response depends on the behavior of the feed flow.

The process is highly unstable, has limitation on the coolant flow rate and has input multiplicity as discussed in (Al-humaizi 2000). These conditions make it very difficult to bring the response to the desired steady state. Therefore, because of input multiplicity and the way each controller is tuned, the controlled process may converge at different steady states. Any attempt to further tune any of these controllers, unstable performance may occur.

## **Conclusions**

Our previous closed loop analysis using a first-principle model for the ethylene to butene-1 dimerization reactor revealed the necessity for a better control design. For this purpose nonlinear control strategies such as fuzzy logic, globally linearizing control and nonlinear model predictive control algorithms were tested for possible stabilization of such a reactor. Application of SISO FLC, GLC and NLMPC algorithms revealed the ability to stabilize the reactor at a low upset in the coolant temperature. At high upsets, saturation of the coolant flow rate occurs degrading the controller performance. This finding is in agreement with that obtained previously. The limitation of the SISO scheme is not related to the control algorithm neither to controller tuning, but rather to the controllability of the process.

Therefore, MIMO and MISO control schemes were tried. In fact, the simulations illustrated that improved control performance can be obtained using the MISO scheme for the PI, FLC and GLC algorithms. On the other hand, the MIMO scheme provided better results when used with the NLMPC algorithm. However, the MIMO scheme suffered from tuning difficulties due to cross loop interaction, which made maintaining both outputs very difficult. A situation gave the MISO scheme more advantage. The inferiority of the MIMO scheme to the MISO scheme when used with the FLC and GLC algorithms depends on the de-coupling nature of those specific control algorithms. Nevertheless, the overall feedback performance of the proposed nonlinear control algorithms was almost comparable to each other and outperforms that obtained using the PI algorithm. The improvement measure is based on the faster settling time for the reactor temperature and on the less offset in the butene yield

## **Nomenclature**

$a$	Tuning parameter for the FLC algorithm
$a_j$	Rate constant for $j$ th reaction, ( $m^3/mole\ s$ ).
$A$	Constant matrix for the FLC defuzzification law
$A_c$	Cooler area for heat transfer ( $m^2$ )
$b$	Tuning parameter for the FLC algorithm
$B$	Constant vector of lower and upper bounds
$b_j$	Rate constant for $j$ th reaction, ( $m^3/mole\ s$ ).
$C$	Constant matrix for linear constraints
$C_p, C_{p_f}, C_{p_w}$	Heat capacity of reactor mixture, feed and water respectively, ( $cal/gm, ^\circ C$ )
$C_4, C_2$	Butene-1 and ethylene concentrations, ( $mole/m^3$ )
$c$	Tuning parameter for the FLC algorithm
$D$	Disturbance estimates
$F$	Reactor fresh feed, ( $m^3/s$ )
$k$	Sampling time, ( $hr$ )
$k_c$	Proportional gain
$k_i$	Adjustable parameter for the GLC algorithm
$K, K_2, K_4, K_6$	Catalyst, and catalyst activator for $C_2, C_4$ and $C_6$ ( $mole/m^3$ )
$K_f$	Catalyst concentration at the fresh feed ( $mole/m^3$ )
$Q$	Reactor product volumetric flow rate ( $m^3/s$ )
$M$	Control horizon
$n_R, n_f, n_y$	Number of FLC rules, FLC fuzzy sets and controlled outputs respectively
$P$	Prediction horizon
$R$	Vector of set point
$r_i$	rates of chain initiation and propagation for $i$ th reaction ( $mole/m^3\ s$ )
$T_c, T_{co}$	Inlet and outlet coolant temperature respectively, ( $^\circ C$ )
$T_f, T_r$	Reactor feed and reference temperature respectively, ( $^\circ C$ )
$T, T_R$	Reactor and recycle temperature respectively ( $^\circ C$ )
$t, t_k$	Time and time at sampling point $k$
$u$	Vector of manipulated variables
$U$	Vector of $M$ future values of $u$
$U_h$	Heat transfer coefficient ( $cal/m^2\ s\ ^\circ C$ )

$V$	Reactor volume ( $m^3$ )
$V_c$	Cooler volume ( $m^3$ )
$x$	State vector
$y$	Output vector
$y_p, y_m$	Plant and model outputs
$W$	Coolant flow rate, ( $kg/s$ )

Greek letter

$\Delta H_r$	Heat of initiation and propagation reactions ( $cal/mole$ )
$\Delta u$	Rate of change for $u$
$\Delta U$	Rate of change for $U$
$\alpha_1, \alpha_2$	Predefined parameters for the GLC algorithm
$\delta$	Location of the membership function center
$\beta$	Recycle ratio
$\Lambda$	Diagonal weight matrix on $\Delta u$
$\Gamma$	Diagonal weight matrix on error signal, $e$
$\lambda$	Diagonal element of $\Lambda$
$\mu$	Membership function
$\tau$	Adjustable parameter for the GLC algorithm
$\tau_I$	Integral time
$\rho, \rho_f$	Mixture and feed densities respectively, ( $kg/m^3$ )

## References

1. Alhumaizi, K. I. "Stability Analysis of the Ethylene Dimerization Reactor for the Selective Production of Butene-1", *ICHEME*, **78**, 492-498 (2000).
2. Ali, E. and K. Alhumaizi, "Temperature Control of Ethylene to Butene-1 Dimerization Reactor", *Ind. Eng. Chem. Res.*, **39**, 1320-1329 (2000).
3. Ali, E.; and E. Zafiriou, "Optimization-Based Tuning of Model Predictive Control with State Estimation" *J. Proc. Cont*, **3**, 97-108 (1993).
4. Ali, E. and S. Elnashaie, "Non-linear Model Predictive Control of Industrial Type IV Fluid Catalytic Cracking (FCC) Units for Maximum Yield", *Ind. & Eng. Chem. Res.*, **36**, 389-398 (1997).
5. Alvarez, J., R. Suarez and A. Sanchez, "Semiglobal Nonlinear Control Based on Complete Input/Output Linearization and its Application to the Start-up of a Continuous Polymerization Reactor", *Chem. Eng. Sci.*, **49**, 3617-3630 (1994).
6. Alvarez, J. "Output-Feedback Control of Nonlinear Plants". *AIChE J.*, **42**, 2540-2554 (1996).
7. Assala, N., F. Viel, and J. P. Gauthier, "Stabilization of Polymerization CSTR Under Input Constraints" *Comp. Chem. Eng.*, **21**, 501-509 (1997).
8. Bernard, J. A. "Use of Rule-Based System for Process Control", *IEEE Control System Magazine*, **8**, 3-13 (1988).
9. Biegler, L. T., and J. B. Rawlings, "Optimization Approach to Nonlinear Model Predictive Control", in proceedings of CPC IV, 543-571 (1991).
10. Braunschweig, S.; Galtier, P.; and Glaize, Y. "ALEXIP", *Revue De Institut Francais Du Petrole*, **47**, 375-383 (1990).
11. Clarke, D. W., Mohtadi, C., and P.S. Tuffs, "Generalized Predictive Control- Part I: the basic algorithm", *Automatica*, **23**, 137-148, (1987).
12. Cutler, C.R., and B. L. Ramaker, "Dynamic Matrix Control- A Computer Control Algorithm", *AIChE 86<sup>th</sup> National Meeting*, Houston, TX (1979).
13. Dadebo, S.; M. Bell; P. Mclellan; and K. McAuley, "Temperature Control of Industrial Gas Phase Polyethylene Reactors", *J. Proc. Cont.*, **7**, 83-96 (1997).
14. Economu, C. G., and M. Morari, "Internal Model Control. 5. Extension to Nonlinear Systems". *Ind. Eng. Chem. Process Des. Dev.*, **25**, 403-411 (1986).
15. Galtier, P. A.; A. A. Forestiere; Y. H. Glaize; and J. P. Wauquire "Mathematical Modeling of Ethylene Oligomerization", *Chem. Eng. Sci.*, **43**, 1855-1860 (1988).

16. Garcia, C.E., and M. Morshedi, "Quadratic Programming Solution of Dynamic Matrix Control (QDMC)", *Chem. Eng. Comm.*, 46, 73-87 (1986).
17. Garrido, R., M. Adroer, and M. Pocj, "Wastewater Neutralization Control Based on Fuzzy Logic Simulation Results", *Ind. Eng. Chem. Res.*, **36**, 1665-1674 (1997).
18. Henson, M. "Nonlinear Model Predictive Control: Current Status and Future Directions", *Comp. Chem. Eng.*, 23, 187-202, (1998).
19. Henson, M. A., D. E. Seborg, "An Internal Model Control Strategy for Nonlinear Systems", *AIChE J.*, **37**, 1065-1081 (1991).
20. Hu, Q., and G. P Rangaiah, "Adaptive Internal Model Control for Nonlinear Processes", *Chem. Eng. Sci.* **54**, 1205-1220 (1999).
21. Hu, Q. and G. P. Rangaiah, "A Time Delay Compensation Strategy for Uncertain Single-Input Single-Output Nonlinear Processes", *Ind. Eng. Chem. Res.*, **38**, 4309-4316 (1999).
22. Inamdar, S. R. and M S. Chiu, "Fuzzy Logic Control of an Unstable Biological Reactor", *Chem. Eng. Technol.* 20, 414-418 (1997).
23. Kendi, T. A., and F. J. Doyle III, "Nonlinear Internal Model Control for Systems with Measured Disturbances and Input Constraints", *Ind. Eng. Chem. Res.*, **37**, 489-505 (1998).
24. Kishimoto, M., T. Yoshida and M. Young, "Application of Fuzzy Expert System to Fermentation Process", *IFAC Workshop PCPI, Osaka, Japan*, 2, (1989).
25. Kravaris, C. and C.B. Chung, "Nonlinear State Feedback Synthesis by Global Input/Output Linearization", *AIChE J.*, **33**, 225-235 (1987).
26. Kravaris, C., R. A. Wright, and J.F. Carrier, "Nonlinear Controllers for Trajectory Tracking in Batch Processes", *Comp. Chem. Eng.*, **13**, 73-82 (1989).
27. Kravaris, C. and C. Kantor, "Geometric Methods for Nonlinear Process Control: 1. Background", *Ind. Eng. Chem. Res.*, **29**, 2295-2310 (1990).
28. Kulkarni, B. D., S. S. Tambe, N. V. Shukla, and P. B. Deshpande, "Nonlinear pH Control", *Chem. Eng. Sci.*, **46**, 995-1003 (1991).
29. Kumar, A. and P. Daoutidis, "Feedback Control of Nonlinear Differential-Algebraic-Equation Systems", *AIChE J.*, **41**, 619-636 (1995).
30. Lee, C.C., "Fuzzy Logic in Control Systems: Fuzzy Logic Controller – Part I", *IEEE Trans. on Sys. Man. And Cybernetics*, **20**, 404-418 (1990a).

31. Lee, C.C., "Fuzzy Logic in Control Systems: Fuzzy Logic Controller – Part II", *IEEE Trans. on Sys. Man. and Cybernetics*, **20**, 419-435 (1990b).
32. Luyben, W. "Tuning Temperature Controllers on Open-loop Unstable Reactors", *Ind. Eng. Chem. Res.*, **37**, 4322-4331 (1998).
33. Mamdani, E. H., "Application of Fuzzy Algorithms for Control of Simple Dynamic Plants", *IEE Proceed.*, **121**(3), 585-588 (1974).
34. Mamdani, E. H., "Application of Fuzzy Logic to Approximate Reasoning Using Linguistic Synthesis, *IEEE Trans. on Computers*, C26(12), 1182-1191, (1977).
35. Morari, M. and J. Lee, "Model Predictive Control: Past, Present and Future", *Comp. Chem. Eng.*, **21**, 667-682 (1999).
36. Parekh, M. and M. Desai, H. H. Lee and R. R. Rhinehart, "Inline Control of Nonlinear pH Neutralization Based on Fuzzy Logic", *IEEE Transaction on Components, Packaging and Mfg. Tech. Part A* 17, 192-201 (1994)
37. Patwardhan, S. C. and K. P. Madhavan, "Nonlinear Internal Model Control Using Quadratic Prediction Models", *Comp. Chem. Eng.*, **22**, 587-601 (1998).
38. Qin, S. J. and T. A. Badgwell, "An Overview of Industrial Model Predictive Control Technology", *Chem. Process Control*, Jan, 1-31, (1996).
39. Qin, S.J. and T.A. Badgwell. "An Overview of Nonlinear Model Predictive Control Applications", In *Nonlinear Model Predictive Control*, edited by F. Allgower and A. Zheng, Birkhauser, Switzerland, (2000)
40. Qin, S.J. and G. Borders, "A Multiregion Fuzzy Logic Controller for Nonlinear Process Control", *IEEE Trans. on Fuzzy Systems*, 2, 74-81, (1994)
41. Ramirez, J. A. "Robust PI Stabilization of a Class of Continuously Stirred-Tank Reactors", *AIChE J.*, **45**, 1992-2000 (1999).
42. Rao, A., V.K. Jayaraman, B.D. Kulkarni, S. Japanwala and P. Shevgaonkar, "Improved Controller Performance with Simple Fuzzy Rules", *Hydrocarbon Processing*, May, 97-100 (1999).
43. Rhinehart, R. R., H. H. Lee and P. Murugan, "Improve Process Control Using Fuzzy Logic", *Chem. Eng. Progress*, **91**(11), 60-65 (1996).
44. Soroush, M., and C. Kravaris, "Discrete-Time Nonlinear Controller Synthesis by Input/Output Linearization", *AIChE*, **38**, 1923-1945 (1992).
45. Soroush, M. "Nonlinear State-Observer Design with Application to Reactors", *Chem. Eng. Sci.*, **52**, 387-404 (1997).

46. Trabzoni, F. "Modeling and Simulation of An Ethylene Dimerization Reactor Dynamics", Msc. Thesis, Chemical Engineering Dept., King Saud University, Riyadh, Saudi Arabia, 1998.
47. Tracy, C. P. and J. F. McGregor, "Nonlinear Adaptive Temperature Control of Multi-Product, Semi-batch Polymerization Reactors", *Comp. Chem. Eng.*, **21**, 1395-1409 (1997).
48. Woo, T.W.; and S. I. Woo, "Kinetics Study of Ethylene Dimerization Catalyzed Over  $Tu(O-nC_4H_9)_4/AlEt_3$ ", *Journal of Catalyst*, **132**, 68-78 (1991).
49. Yen, J. and Langari, R. *Fuzzy Control*, Prentice Hall, New Jersey, 1999.
50. Zadeh, L. A., "Fuzzy Sets", *Information Control*, **8**, 330-353 (1965).

### **Figure captions**

Figure 1: Schematic of the Dimerization reaction process

Figure 2: Steady state bifurcation diagram

Figure 3: Open-loop simulation of the reactor temperature for two values of  $T_c$ .

Figure 4: Block diagram of the FLC algorithm.

Figure 5: Gaussian fuzzy set used in this paper

Figure 6: Example of clipped output membership function

Figure 7: Block diagram for the GLC algorithm

Figure 8: Closed loop response to step changes in  $T_c$ : +4 °C (solid), +6 °C (dashed) using SISO PI control algorithm.

Figure 9: Closed loop response to step change in  $T_c$  of +6 °C using PI control algorithm, Dashed line: MISO scheme, solid line: MIMO scheme.

Figure 10: Closed loop response to step changes in  $T_c$  using SISO FLC algorithm, (a,b):  $\Delta T_c = +4$  °C, (c,d):  $\Delta T_c = +6$  °C

Figure 11: Closed loop response to step change in  $T_c$  of +6 °C using FLC algorithm. MIMO (solid), MISO (dashed)

Figure 12: Closed loop response to step changes in  $T_c$  using SISO GLC algorithm: +4 °C (solid), +6 °C (dashed).

Figure 12: Closed loop response to step changes in  $T_c$  using SISO GLC algorithm: +4 °C (solid), +6 °C (dashed).

Figure 14: Closed loop response to step change in  $T_c$  of +4 °C (solid), +6°C (dashed) using SISO NLMPC.

Figure 15: Closed loop response to step change in  $T_c$  of +6 °C using MISO NLMPC (dashed), MIMO NLMPC (solid).

Table 1: Dimerization reactor design parameters

$C_p = 0.55 \text{ cal/g.}^\circ\text{C}$	$C_{2f} = 25000 \text{ mole/m}^3$	$-\Delta H_{r1} = -25000 \text{ cal/mole}$
$C_{pf} = 0.55 \text{ cal/g.}^\circ\text{C}$	$K_f = 1.25 \text{ mole/m}^3$	$-\Delta H_{r2} = -25000 \text{ cal/mole}$
$V_c = 50 \text{ m}^3$	$\rho = 500 \text{ kg/m}^3$	$V = 500 \text{ m}^3$
$T_r = 25^\circ\text{C}$	$UA = 27500 \text{ cal/mole s}$	$C_{pw} = 1.0 \text{ cal/g.}^\circ\text{C}$

Table 2: Favorable operating condition

Variable	$W$ (kg/s)	$F_{X1000}$ ( $\text{m}^3/\text{s}$ )	$\beta$	$T_f$ ( $^\circ\text{C}$ )	$K_f$ ( $\text{mole/m}^3$ )	$T, T_R$ ( $^\circ\text{C}$ )	$C_2$ ( $\text{mole/m}^3$ )	$C_4$ ( $\text{mole/m}^3$ )
Value	500	4.0	0.02	30.0	1.25	67, 43	1065	8700

Table 3: Rule base, mathematical representation

no.	Fuzzy rule	Results (Conclusion)
R1	If e is LP & Δe is LP then Δu is LP	$\mu_{1,1}(\Delta u) = \min(\mu_1(e), \mu_1(\Delta e))$
R2	If e is SP & Δe is SP then Δu is SP	$\mu_{2,2}(\Delta u) = \min(\mu_2(e), \mu_2(\Delta e))$
R3	If e is SN & Δe is SN then Δu is SN	$\mu_{4,3}(\Delta u) = \min(\mu_4(e), \mu_4(\Delta e))$
R4	If e is LN & Δe is LN then Δu is LN	$\mu_{5,4}(\Delta u) = \min(\mu_5(e), \mu_5(\Delta e))$
R5	If e is LP & Δe is ZE then Δu is SP	$\mu_{1,5}(\Delta u) = \min(\mu_1(e), \mu_3(\Delta e))$
R6	If e is SP & Δe is ZE then Δu is SP	$\mu_{2,6}(\Delta u) = \min(\mu_2(e), \mu_3(\Delta e))$
R7	If e is SN & Δe is ZE then Δu is SN	$\mu_{4,7}(\Delta u) = \min(\mu_4(e), \mu_3(\Delta e))$
R8	If e is LN & Δe is ZE then Δu is SN	$\mu_{5,8}(\Delta u) = \min(\mu_5(e), \mu_3(\Delta e))$
R9	If e is LP & Δe is SN then Δu is ZE	$\mu_{3,9}(\Delta u) = \min(\mu_1(e), \mu_4(\Delta e))$
R10	If e is SP & Δe is SN then Δu is ZE	$\mu_{3,10}(\Delta u) = \min(\mu_2(e), \mu_4(\Delta e))$
R11	If e is SN & Δe is SP then Δu is ZE	$\mu_{3,11}(\Delta u) = \min(\mu_4(e), \mu_2(\Delta e))$
R12	If e is LN & Δe is SP then Δu is ZE	$\mu_{3,12}(\Delta u) = \min(\mu_5(e), \mu_2(\Delta e))$
R13	If e is LP & Δe is SP then Δu is LP	$\mu_{1,13}(\Delta u) = \min(\mu_1(e), \mu_2(\Delta e))$
R14	If e is SP & Δe is LP then Δu is LP	$\mu_{1,14}(\Delta u) = \min(\mu_2(e), \mu_1(\Delta e))$
R15	If e is SN & Δe is LN then Δu is LN	$\mu_{5,15}(\Delta u) = \min(\mu_4(e), \mu_5(\Delta e))$
R16	If e is LN & Δe is SN then Δu is LN	$\mu_{5,16}(\Delta u) = \min(\mu_5(e), \mu_4(\Delta e))$
R17	If e is LP & Δe is LN then Δu is SN	$\mu_{4,17}(\Delta u) = \min(\mu_1(e), \mu_5(\Delta e))$
R18	If e is SP & Δe is LN then Δu is SN	$\mu_{4,18}(\Delta u) = \min(\mu_2(e), \mu_5(\Delta e))$
R19	If e is SN & Δe is LP then Δu is SP	$\mu_{2,19}(\Delta u) = \min(\mu_4(e), \mu_1(\Delta e))$
R20	If e is LN & Δe is LP then Δu is SP	$\mu_{2,20}(\Delta u) = \min(\mu_5(e), \mu_1(\Delta e))$
R21	If e is ZE & Δe is ZE then Δu is ZE	$\mu_{3,21}(\Delta u) = \min(\mu_3(e), \mu_3(\Delta e))$
R22	If e is ZE & Δe is LN then Δu is SN	$\mu_{4,22}(\Delta u) = \min(\mu_3(e), \mu_5(\Delta e))$
R23	If e is ZE & Δe is LP then Δu is SP	$\mu_{2,23}(\Delta u) = \min(\mu_3(e), \mu_1(\Delta e))$
R24	If e is ZE & Δe is SN then Δu is ZE	$\mu_{3,24}(\Delta u) = \min(\mu_3(e), \mu_4(\Delta e))$
R25	If e is ZE & Δe is SP then Δu is ZE	$\mu_{3,25}(\Delta u) = \min(\mu_3(e), \mu_2(\Delta e))$

Table 4: performance comparison for the tested controllers for  $\Delta T_c = + 6 \text{ }^\circ\text{C}$

<i>Algorithm</i>	<i>Structure</i>	<i>Overshoot (<math>^\circ\text{C}</math>)</i>	<i>Settling time (hr)</i>	<i>Offset (<math>\text{mole/m}^3</math>)</i>
PI	SISO	73.3	50	143
	MISO	69.4	30	26
	MIMO	73.2	8	73
FLC	SISO	Oscillatory	Oscillatory	Oscillatory
	MISO	69.6	5	0
	MIMO	73.5	8	67
GLC	SISO	73.9	19	74
	MISO	68.8	5	7
	MIMO	73.9	12	74
NLMPC	SISO	72.2	19	71
	MISO	68.8	4.5	9
	MIMO	68.2	4.5	4

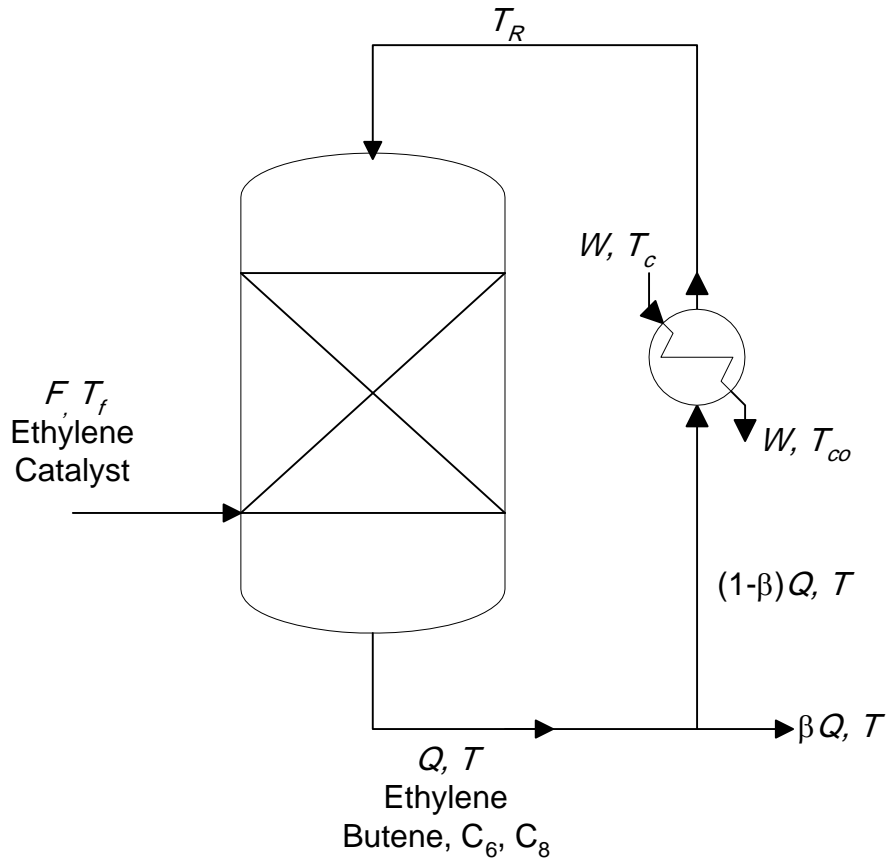


Figure 1: Schematic of the Dimerization reaction process

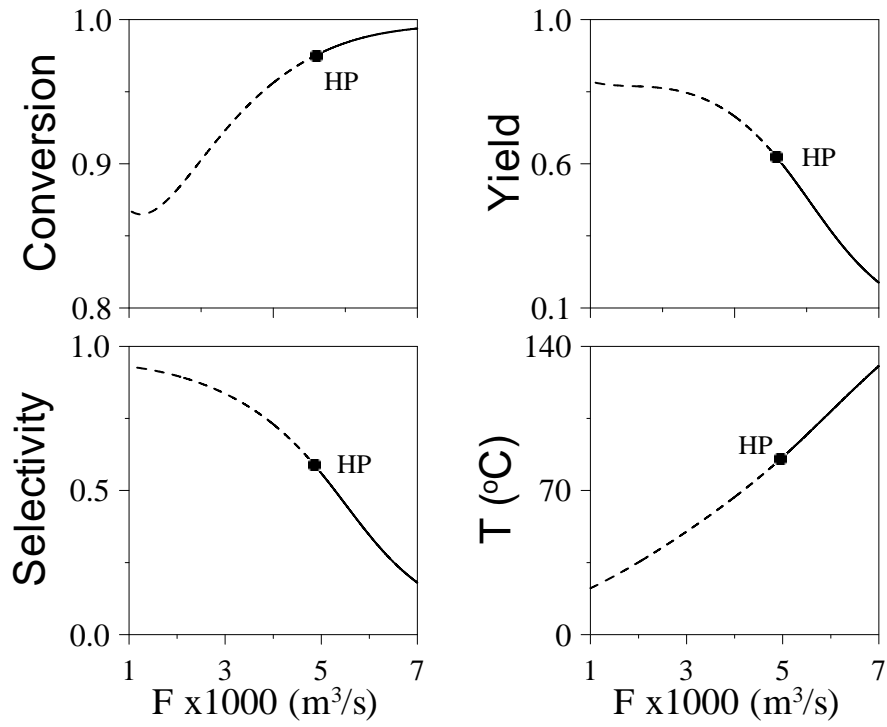


Figure 2: Steady state bifurcation diagram

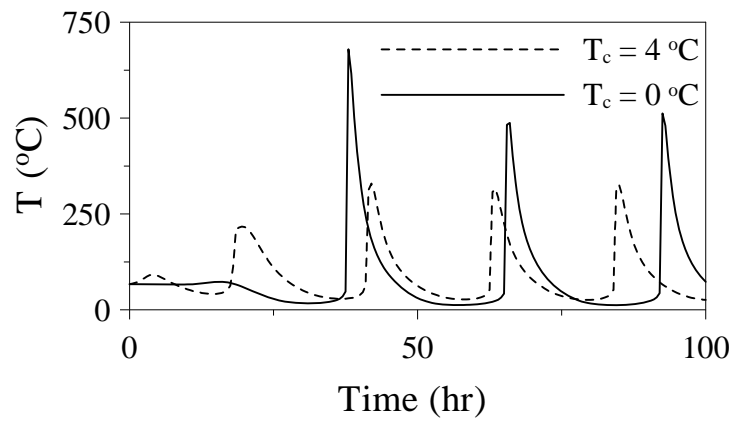


Figure 3: Open-loop simulation of the reactor temperature for two values of  $T_c$ .

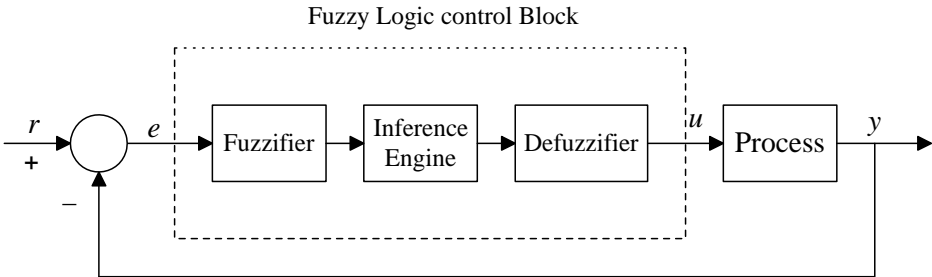


Figure 4: Block diagram of the FLC algorithm

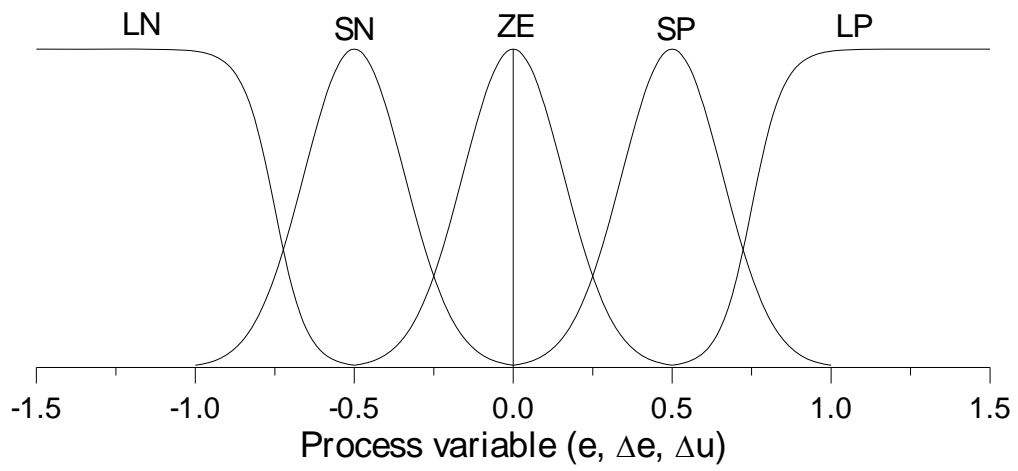


Figure 5: Gaussian fuzzy set used in this paper

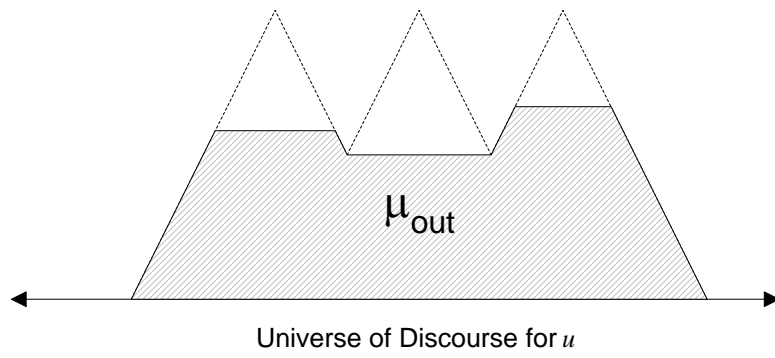
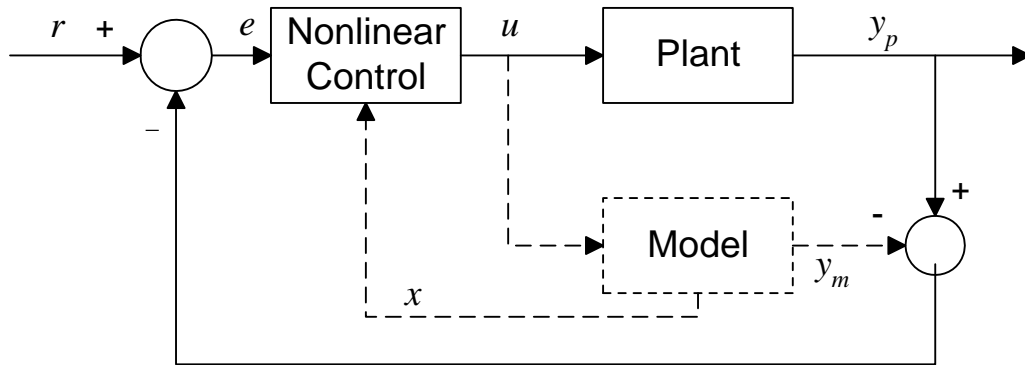


Figure 6: Example of clipped output membership function



**Figure 7: Block diagram for the GLC algorithm**

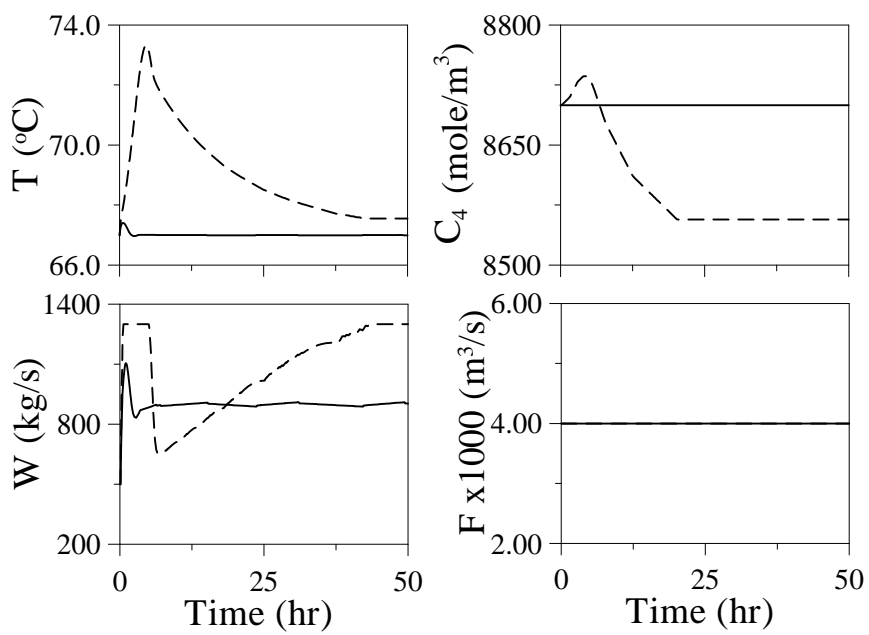


Figure 8: Closed loop response to step changes in  $T_c$ :  $+4^{\circ}\text{C}$  (solid),  $+6^{\circ}\text{C}$  (dashed) using SISO PI control algorithm.

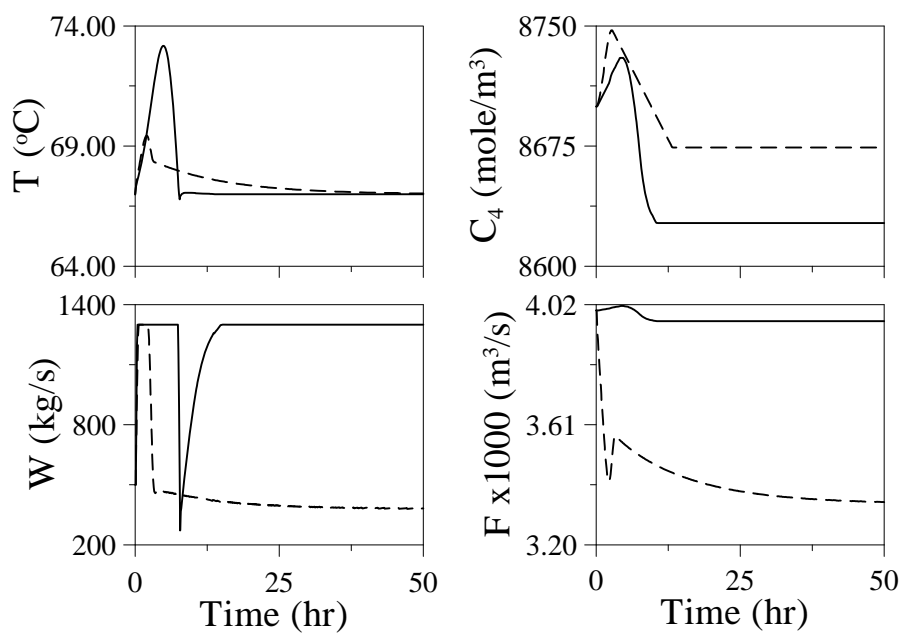


Figure 9: Closed loop response to step change in  $T_c$  of +6 °C using PI control algorithm, Dashed line: MISO scheme, solid line: MIMO scheme.

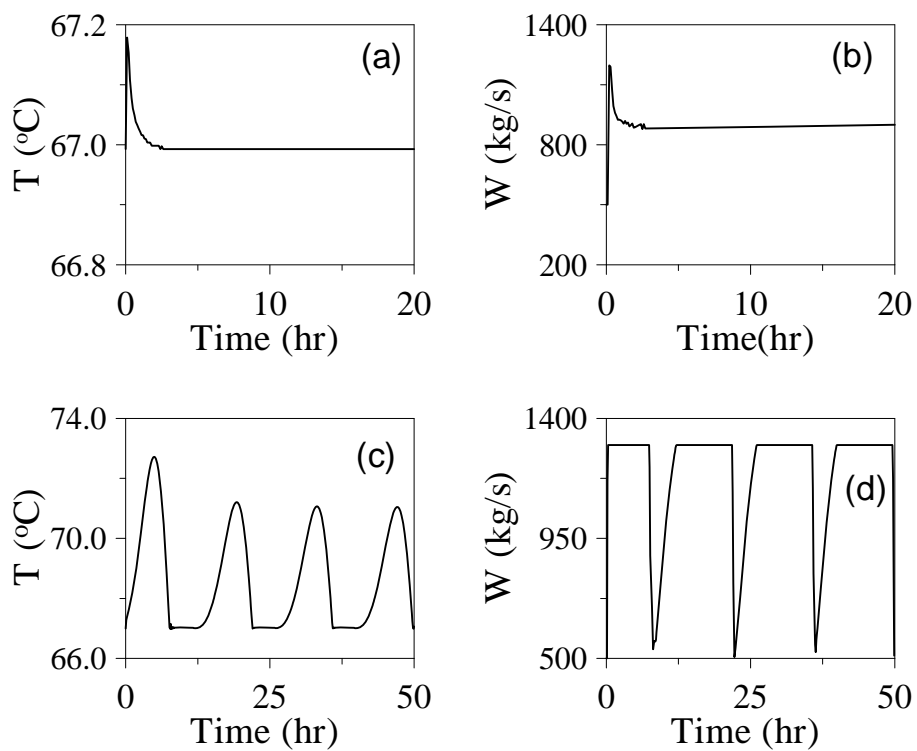


Figure 10: Closed loop response to step changes in  $T_c$  using SISO FLC algorithm, (a,b):  $\Delta T_c = +4^\circ\text{C}$ , (c,d):  $\Delta T_c = +6^\circ\text{C}$

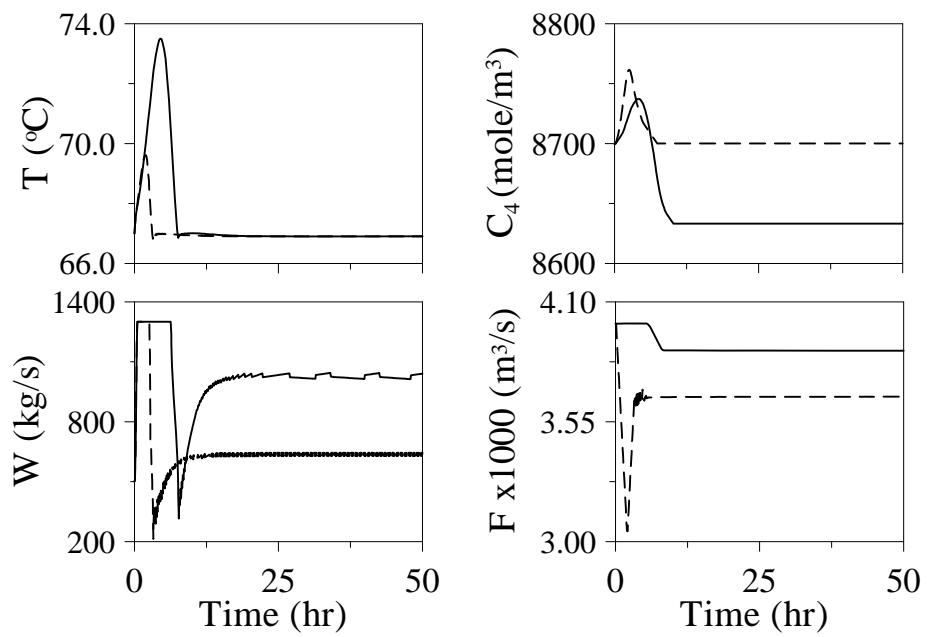


Figure 11: Closed loop response to step change in  $T_c$  of  $+6^\circ\text{C}$  using FLC algorithm. MIMO (solid), MISO (dashed)

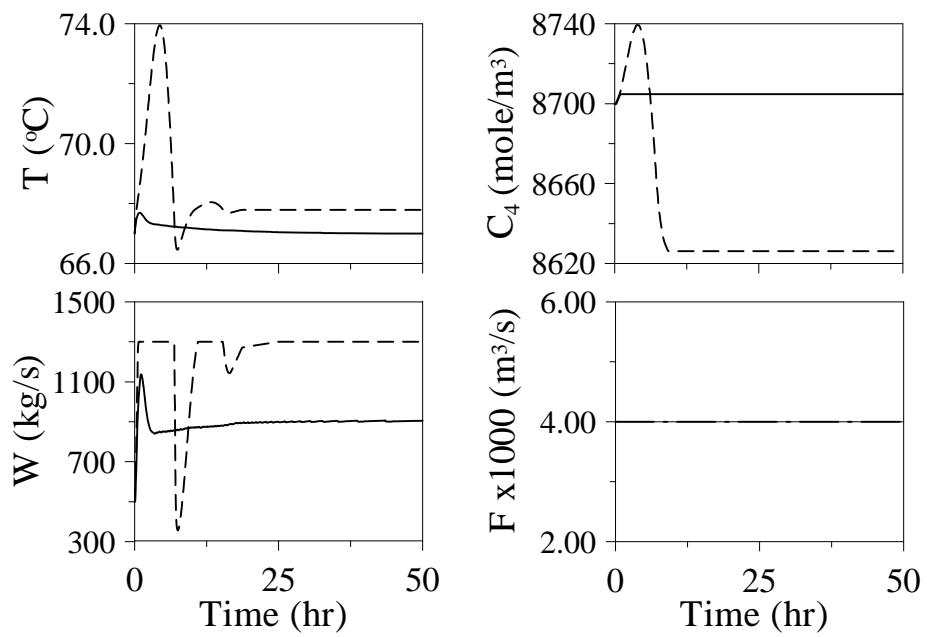


Figure 12: Closed loop response to step changes in  $T_c$  using SISO GLC algorithm: +4 °C (solid), +6 °C (dashed).

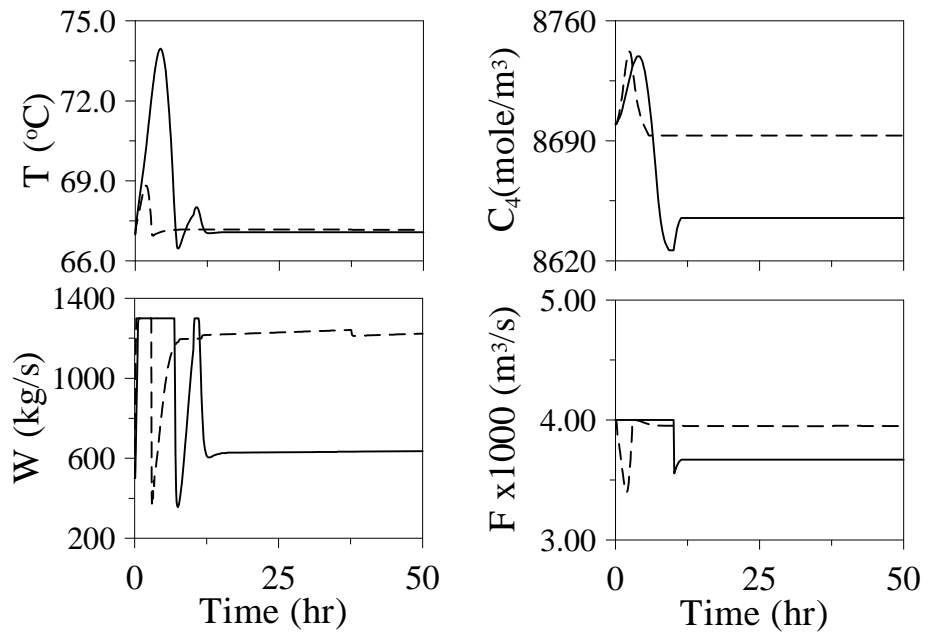


Figure 13: Closed loop response to step change in  $T_c$  of +6 °C using MIMO (solid), MISO (dashed) GLC algorithms.

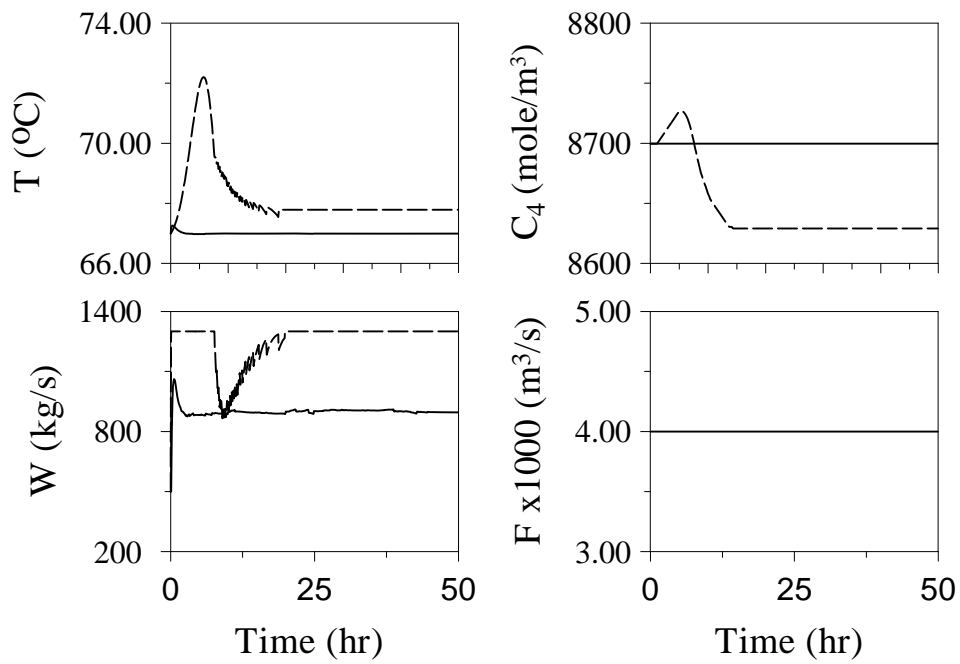


Figure 14: Closed loop response to step change in  $T_c$  of  $+4^\circ\text{C}$  (solid),  $+6^\circ\text{C}$  (dashed) using SISO NLMPC.

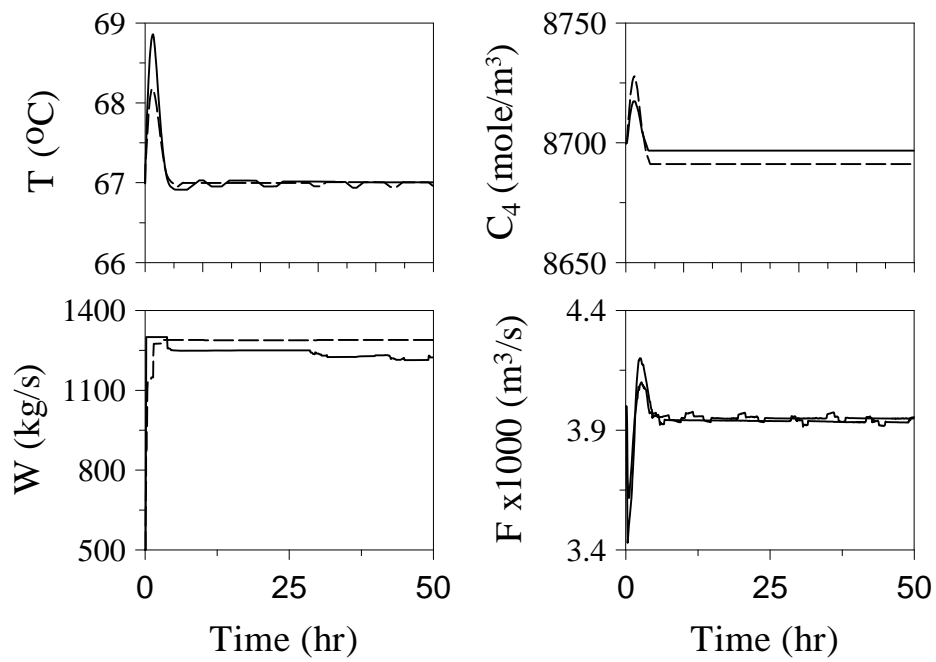


Figure 15: Closed loop response to step change in  $T_c$  of +6 °C using MISO NLMPC (dashed), MIMO NLMPC (solid).